

On Increasing Energy Autonomy for a One-Legged Hopping Robot

Evangelos Papadopoulos, Nicholas Cherouvim
Department of Mechanical Engineering
National Technical University of Athens
15780 Athens, Greece
 egpapado@central.ntua.gr, ndcherouvim@hotmail.com

Abstract - In this paper it is shown that, for a one-legged robot, there exists a particular passive gait, of all those possible, for which the dissipated energy per meter of travel is minimized. An analytical method is used to identify the optimal gait. A SLIP model of the robot is used to simplify the dynamics. Both mechanical and electrical losses are taken into account. A numerical analysis of a complete robot model follows, to evaluate the accuracy of the analytical prediction. Finally, the limitations imposed by a torque limited motor, with regard to the optimal gait, are studied.

Index Terms - Hopping robot, SLIP model, passive hopping.

I. INTRODUCTION

Legged robots started being developed only about two decades ago. Large parts of this planet, and others, are comprised of anomalous terrain that makes locomotion with wheeled vehicles impossible. On the other hand, legged robots have the potential of being able to handle steep inclines and negotiate obstacles. The fact that legged robots do not come into contact with all the points of the ground they transverse, as in the case of wheeled vehicles, facilitates their motion through rough terrain.

Legged robots may be categorized according to the number of their legs, their type of stability (static, dynamic), their passive or active nature, and the type and number of actuators they may possess.

Robots with two [1], [3], four [1], [4], six [5] and eight legs and even robots combining legs and wheels have been built. One-legged robots may either move in three dimensions, [1], or be constrained to the plane, [6], as is the model studied in this paper.

Depending on whether the robot is statically balanced at every point in time, or merely executes a cyclic movement that is stable as a whole, a robot may be characterized as statically or dynamically stable. Naturally, one-legged robots are always dynamically stable, since they cannot be statically stable with one leg.

Legged robots may be distinguished as to whether or not they are active, that is whether they make use of actuators to move, or not [2]. In the past, both hydraulic, [1], [3], and pneumatic actuators, [6] have been used in active robots. In these cases, the robot is often connected to a stationary base that feeds the robot with power. This physical connection acts as a constant disturbance on the robot's movement, while also restricting the distance it may travel. On the other hand,

electric motors have been used more recently, [4], [5], that may be powered by batteries situated on-board the robot. It is obvious that electric motors offer the means of driving the robot while achieving autonomy. However, because powerful motors are heavy, as are batteries that store larger amounts of energy, it is imperative that the robot moves in an optimum way from an energy consumption point of view.

The analysis in this paper is based on the SLIP (Spring Loaded Inverted Pendulum) model. This model is frequently used to study legged robots and is composed of a point mass attached on a spring that is free to rotate around its point of contact with the ground. A similar model has been used by Dummer and Berkemeier to analyze the passive dynamics and control of a one legged robot, [7]. An approximate stance map for the SLIP model has been found by Schwind and Koditschek, [8]. Until now, little if any work has incorporated energy losses into the SLIP model.

Passive running has also been studied by Raibert and Buehler. Energy savings of 93% are reported, when passive running is used [2]. It is now generally accepted that passive running will lead to the least energy consumption. However, this paper differs from previous work in that it points out that all passive gaits do not lead to the same amount of dissipated energy, and that running a robot close to its passive motion does not guarantee the least energy consumption. The energy dissipated by the robot during its motion has generally not been considered in previous studies.

In this paper, it is analytically shown which passive gait, of the many possible, leads to the least dissipated energy per meter of travel. Both the mechanical and electrical energy dissipated during the robot's motion is considered. Using a SLIP model and making some mild assumptions, an analytical prediction for the optimal gait is found. To verify the prediction, numerical simulations are carried out. Finally, the effects on the optimal gait imposed by a torque-limited actuator are studied.

II. ROBOT DYNAMICS

The SLIP physical model is shown in Fig. 1. The model is comprised of a body of point mass m , a massless leg with a rest length L and a spring in the leg of stiffness k . The leg forms an angle θ with the vertical, while the length of the leg at any moment in time is l . For the analytical study, the pitching of the body and inertia of the leg are ignored, and θ is thought to be small. Also, there is no slipping of the foot during stance. To verify analytical results, simulations of a *full*

model with pitching and leg inertia are employed.

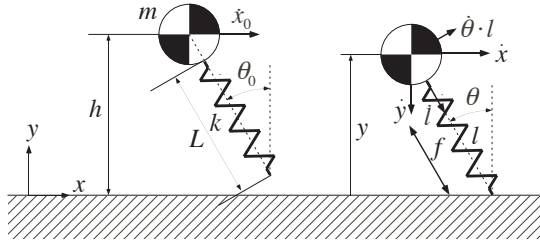


Fig. 1. The SLIP physical model at the beginning of the motion and at a typical point of the stance phase.

The system has losses, due to viscous friction at the leg with a viscous coefficient of b . To supplement the loss of energy, the robot has a motor that actuates the leg. When moving, the robot goes through a stance and a flight phase, see Fig. 2. During stance, the robot center of mass (CM) covers a distance of x_s , and a distance of x_f during flight, reaching an apex height of h .

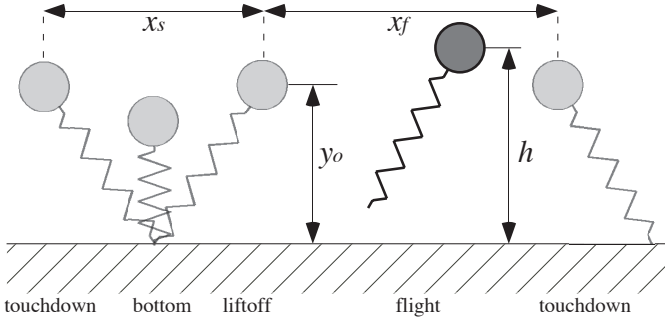


Fig. 2. Phases of the robot motion.

The equations of motion for the robot during stance may be found using a Lagrangian approach:

$$\begin{aligned} ml^2\ddot{\theta} + 2ml\dot{l}\dot{\theta} - mgl\sin\theta &= 0 \\ ml\ddot{l} - ml\dot{\theta}^2 + k(l-L) + mg\cos\theta + b\dot{l} &= f \end{aligned} \quad (1)$$

where f is the force the actuator exerts on the leg spring.

During flight, the robot is under the influence of gravity only. Its position may be determined by the mass horizontal position x and distance from the ground y . Therefore, the equations during flight are:

$$\begin{aligned} \ddot{x} &= 0 \\ \ddot{y} &= -g \end{aligned} \quad (2)$$

where g is the acceleration of gravity.

III. PASSIVE RUNNING AND DISSIPATED ENERGY

If the robot has no losses, then sets of initial conditions may be found for which the robot executes a passive motion, providing the leg is swung forward during flight [1]. In this ideal case, the robot may move with zero energy consumption. However, in reality, friction does exist in the leg, so the robot will not perform more than a few hops with these initial conditions. Therefore a completely passive motion of the robot is not possible, and a motor is required for the robot to execute a sustainable gait. The motor may exert a force f on the leg

that exactly compensates friction. The force f that compensates the friction force f_{fr} is:

$$f = f_{fr} = b \cdot \dot{l} \quad (3)$$

where \dot{l} is the velocity of the body in the direction of the leg. It is clear that the friction term in the equations of motion, see Eq. (1), is now canceled by the force f . This means that, using sets of initial conditions that yield a passive motion for the lossless system, and a friction compensating motor, the robot will execute an active gait very close to the passive gait. In such a case, the robot may be studied as in the frictionless case, and the only energy required to sustain the motion is the energy dissipated due to friction in the leg.

It is has been well shown that passive running is the most efficient type of running. However, depending on the initial conditions, the characteristics of a passive gait, such as the time the robot is on the ground during a cycle, as well as the robot's speed, will vary. Our work showed that the energy dissipated during each passive gait varies and that the differences for various gaits are considerable. Hence, it is necessary to identify the gait for which the dissipated energy per meter of travel is the least.

A particular gait is defined by a set of initial conditions such as the initial height h of the body from the ground, the horizontal velocity \dot{x}_0 of the CM and the leg angle θ_0 at touchdown. For given values of parameters h and θ_0 , the velocity \dot{x}_0 is uniquely defined for a 'passive' gait, in a normal working range. If only the value of the apex height h is restrained, the robot may execute a wide range of 'passive' gaits with different values of the velocity \dot{x}_0 , for various values of the leg angle at touchdown θ_0 . It will be shown that for a particular value of θ_0 , the losses of the robot per meter of travel are minimized, for a given h and \dot{x}_0 .

The losses of the robot are due to the friction in the leg, and the motor's ohmic resistance r . The friction force is given in Eq. (3), and the losses due to friction are:

$$P_{fr} = b \cdot \dot{l}^2 \quad (4)$$

The force f exerted on the leg by the motor is:

$$f = g_e \cdot \tau_m \quad (5)$$

where g_e is the transformation ratio of the mechanism that converts the revolute motion of the motor to the linear motion of the leg, τ_m is the motor torque output. Neglecting mechanical losses in the motor, the torque τ_m of the motor is:

$$\tau_m = k_m i \quad (6)$$

where k_m is the torque constant of the motor, i is the current of the motor. The ohmic losses of the motor are:

$$P_m = i^2 r \quad (7)$$

where r is the motor resistance. Eqs. (3), (5), (6) give:

$$P_m = \frac{b^2 r}{g_e^2 k_m^2} \dot{l}^2 \quad (8)$$

Therefore, the total losses are:

$$P = P_m + P_{fr} = b_{tot} \dot{l}^2 \quad (9)$$

where $b_{tot} = b + b^2 r (g_e k_m)^{-2}$.

IV. ANALYTICAL APPROACH

It is attempted to compute analytically the best operating gait of the robot, for which the average losses of energy per meter of travel, \hat{e} , are minimized. The gait is defined by the angle of the leg at touchdown θ_0 , for a given apex height h .

The quantity \hat{e} is defined as the total energy losses during one stance, over the distance covered during one stance and one flight period. During the flight phase there are no losses since the leg may be brought forward with zero torque. If e_s is the energy lost during stance then:

$$\hat{e} = \frac{e_s}{(x_s + x_f)} \quad (10)$$

For the optimum angle $\theta_{0,opt}$, for which the losses per meter will be minimized, the derivative of \hat{e} with respect to θ_0 will be equal to zero, so:

$$\frac{d\hat{e}}{d\theta_0} = 0 \quad (11)$$

Eq. (11) is the equation which will provide the optimum θ_0 . Below, (') denotes the derivative with respect to θ_0 . Taking Eq. (10) into account, Eq. (11) becomes:

$$\frac{e'_s(x_s + x_f) - e_s(x'_s + x'_f)}{(x_s + x_f)^2} = 0 \text{ or } \frac{e'_s}{e_s} = \frac{x'_s + x'_f}{x_s + x_f} \quad (12)$$

Since the motor of the robot exactly compensates the friction force in the leg, the robot's movement is described by the unperturbed equations of motion:

$$\begin{aligned} ml^2\ddot{\theta} + 2ml\dot{l}\cdot\dot{\theta} - mgl\sin\theta &= 0 \\ m\ddot{l} - ml\dot{\theta}^2 + k(l - L) + mg\cos\theta &= 0 \end{aligned} \quad (13)$$

The energy lost during stance is:

$$e_s = \int_0^{T_s} P_{tot} dt = b_{tot} \int_0^{T_s} \dot{l}^2 dt = b_{tot} P \quad (14)$$

where T_s is the duration of the stance phase and:

$$P = \int_0^{T_s} \dot{l}^2 dt \quad (15)$$

Taking into account Eqs. (14), and (15), Eq. (12) which will provide $\theta_{0,opt}$, may be written as:

$$\frac{p'}{p} = \frac{x'_s + x'_f}{x_s + x_f} \quad (16)$$

Eq. (16) shows that the optimum angle of touchdown is independent of the leg damping coefficient. For the optimum angle to be calculated from Eq. (16), the distances x_f and x_s must be expressed as functions of the touchdown angle θ_0 .

A. Expressing x_f as a function of θ_0 : The gaits considered have the same apex height h . The height of the body of the robot at liftoff, see Fig. 2, is:

$$y_0 = L\cos\theta_0 \quad (17)$$

If the liftoff angle is considered to be small, then:

$$y_0 \approx L \quad (18)$$

During flight, the robot is under the influence of gravity only. The duration of flight can be found as:

$$T_f = 2\sqrt{2h_d/g} \quad (19)$$

where,

$$h_d = h - y_0 \geq 0 \quad (20)$$

At liftoff, the speed of the body of the robot in the horizontal direction is, see Fig. 1:

$$\dot{x}_{lo} = \dot{\theta}_{lo}L\cos\theta_0 - \dot{l}_{lo}\sin\theta_0 \quad (21)$$

where $\dot{\theta}$ is the angular velocity, and the subscript (lo) denotes the value of a quantity at liftoff.

It is presumed that the leg velocity \dot{l} does not significantly contribute to the horizontal velocity at liftoff. Mathematically, this means that the second term of Eq. (21) is small in comparison to the first. If this approximation is made, and because θ_0 is small and for a symmetric gait $\dot{\theta}_{lo} = \dot{\theta}_0$, Eq. (21) may be written as:

$$\dot{x}_{lo} = \dot{\theta}_0L \quad (22)$$

Since the robot travels with a constant horizontal speed of \dot{x}_{lo} during flight, the distance x_f it covers during flight is, using the flight duration in Eq. (19):

$$x_f = 2L\dot{\theta}_0\sqrt{2h_d/g} \quad (23)$$

From the linearized equations of motion, it can be found that approximately (see Appendix B):

$$\dot{\theta}_0 = -\theta_0 2\sqrt{k/(m\pi^2)} \quad (24)$$

Taking into account Eq. (24), Eq. (23) gives an expression for the x_f distance covered during flight:

$$x_f = -\theta_0 4L\sqrt{2kh_d}/(\pi\sqrt{mg}) = a_1 \cdot \theta_0 \quad (25)$$

where a_1 does not depend on θ_0 .

B. Expressing x_s as a function of θ_0 : From Fig. 2 it may be seen that the distance the robot covers during stance is:

$$x_s = -2L\sin\theta_0 = a_2\theta_0 \quad (26)$$

where a_2 does not depend on θ_0 .

C. Expressing p as a function of θ_0 : Using Eqs. (25) and (26), Eq. (16) gives:

$$\frac{p'}{p} = \frac{a_2 + a_1}{(a_2 + a_1)\theta_0} = \frac{1}{\theta_0} \quad (27)$$

The leg speed, as derived from the linearized equation for the leg, is (see Appendix A for more detail):

$$\dot{l}(t) = \dot{l}_0\cos(\sqrt{k/m}\cdot t) - g\sqrt{m/k}\sin(\sqrt{k/m}\cdot t) \quad (28)$$

where \dot{l}_0 is the leg speed at touchdown. Using Eq. (28), (14b), p may be calculated as:

$$\begin{aligned} p = \frac{1}{4a_3^3} [2a_3(T_s(g^2 + a_3^2\dot{l}_0^2) - g\dot{l}_0(1 - \cos(2a_3T_s))) \\ + (-g^2 + a_3^2\dot{l}_0^2)\sin(2a_3T_s)] \end{aligned} \quad (29)$$

where $a_3 = \sqrt{k/m}$.

From Eq. (28), the stance time can be found to be approximately (see Appendix A for more detail):

$$T_s \approx \pi \sqrt{m/k} \quad (30)$$

Taking into account Eq. (30), the following are true:

$$\begin{aligned} \cos(2a_3 T_s) &\approx \cos(2\pi) = 1 \\ \sin(2a_3 T_s) &\approx \sin(2\pi) = 0 \end{aligned} \quad (31)$$

Substituting Eq. (30), (31), into Eq. (29), p is given by:

$$p = \frac{1}{2} (m/k)^{3/2} (g^2 + l_0^2 k/m) \quad (32)$$

To calculate the optimum angle of touchdown $\theta_{0,opt}$ from Eq. (27), l_0 must first be expressed in terms of θ_0 .

D. Expressing l_0 as a function of θ_0 : If \dot{y}_0 is the vertical speed of the CM at touchdown, then the duration of flight T_f is:

$$T_f = -2 \frac{\dot{y}_0}{g}, \text{ so } \dot{y}_0 = -g \frac{T_f}{2} \quad (33)$$

From Fig. 1, the vertical speed at touchdown \dot{y}_{td} is:

$$\dot{y}_0 = \dot{l}_0 \cos \theta_0 + \dot{\theta}_0 L \sin \theta_0 \quad (34)$$

or, assuming again that θ_0 is small:

$$\dot{y}_0 = \dot{l}_0 + \dot{\theta}_0 L \theta_0 \quad (35)$$

From Eq. (33), (35) it can be found that:

$$\dot{l}_0 = a_4 \theta_0^2 + a_5 \quad (36)$$

where $a_4 = -2L\sqrt{k/m}/\pi$, $a_5 = -\sqrt{2gh_d}$.

E. Calculation of optimal touchdown angle θ_0 : Substituting Eq. (36) into Eq. (32), the quantity p becomes a function dependent only on θ_0 . Eq. (27), from which the optimum θ_0 will be determined, then takes the form of a fourth order equation:

$$n\theta_0^4 + q\theta_0^2 + w = 0 \quad (37)$$

where

$$n = -\frac{12}{\pi^2} \frac{k^2}{m^2} L^2, q = -\sqrt{\frac{k}{m}} \frac{2L}{m} \sqrt{2gh_d}, w = g^2 + 2gh_d \frac{k}{m}.$$

From Eq. (37), $\theta_{0,opt}$ is calculated:

$$\theta_{0,opt}^2 = (-q \pm d)/(2n) \quad (38)$$

where:

$$d^2 = q^2 - 4nw = \frac{104}{\pi^2} L^2 \left(\frac{k}{m}\right)^3 gh_d + \frac{48}{\pi^2} L^2 \left(\frac{k}{m}\right)^2 g^2 \quad (39)$$

In Eq. (39), the second term is substantially smaller than the first term, since $k/m \gg 1s^{-2}$. So:

$$d \approx L \sqrt{104gh_d} \sqrt{k/m}^3 / \pi$$

From Eq. (38), the optimum angle of touchdown $\theta_{0,opt}$ is:

$$\theta_{0,opt} = 0.9824 \sqrt{\frac{mgh_d}{kL^2}} \approx 4 \sqrt{\frac{mgh_d}{kL^2}} \quad (40)$$

Eq. (40) provides a simple expression for the optimal angle θ_0 , for a given apex height h . This expression can be useful in robot design. Specifically, having chosen a reasonable apex height h , the parameters m , k , L , of the robot

may be chosen so that the optimal θ_0 has a value that is acceptable, i.e. the foot does not slip during stance, and the resulting motion is not too fast.

V. NUMERICAL APPROACH

To verify the formula derived above, simulations were carried out in MATLAB by numerically solving the full nonlinear dynamics of a robot with pitching of the body and leg inertia. A wide range of robot parameters was used. Specifically, having specified an apex height of 0.7m, the parameter of the body mass of the robot was varied in the range $m=(5 \text{ kg}, 25 \text{ kg})$, while the parameter of the spring stiffness was varied in the region $k=(5000 \text{ N/m}, 20000 \text{ N/m})$. The rest length of the leg was kept as $L=0.5 \text{ m}$. In Table 1, the relative error s of the prediction of the analytical formula in Eq. (40) against the prediction of the numerical simulation is shown, for various sets of parameters.

Table 1. Analytical approximation relative error for an apex height of 0.7 m.

m (kg)	k (kN/m)	L (m)	s (%)
5	4	0.5	19.5
5	20	0.5	15.8
20	10	0.5	17.7
20	20	0.5	19.6
30	15	0.5	17.8
30	20	0.5	17.7

As can be seen, the error is approximately constant and equal to about 0.18. Because the error is constant, the formula in Eq. (40) may be modified with the addition of a constant factor of 1.2, so that the average error is close to zero. Therefore, the modified formula for the calculation of the optimum touchdown angle for a specified maximum hopping height is:

$$\theta_{0,opt} = 1.2 \cdot 4 \sqrt{\frac{mgh_d}{kL^2}} \quad (41)$$

Simulations for apex heights in the range of (0.6-0.85) m, showed minimal deviations from the predictions of Eq. (41). Simulations were also carried out for a robot with $m=10 \text{ kg}$, $k=10000 \text{ N/m}$, $L=0.5 \text{ m}$, body inertia $i_b=0.5 \text{ kg m}^2$, leg inertia $i_l=0.05 \text{ kg m}^2$, for apex heights of $h=0.57 \text{ m}$ and $h=0.70 \text{ m}$, $b=5 \text{ kg/s}$, $k_m=0.04 \text{ Nm/A}$, $g_c=50 \text{ rad/m}$, $r=4 \Omega$. The consumed energy per meter \hat{e} is shown in Fig. 3. Eq. (41) predicts an optimum angle of $\theta_{0,opt} = 15.6 \text{ deg}$ for the first height and $\theta_{0,opt} = 20.4 \text{ deg}$ for the second height. It can be seen from Fig. 3 that the true optimum angles are about $\theta_{0,opt} = 15 \text{ deg}$ and $\theta_{0,opt} = 20 \text{ deg}$ respectively.

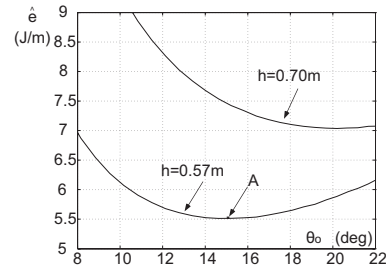


Fig. 3. Energy used per meter for two apex heights.

To validate the result from the above simulations, the robot was simulated in addition with the Working Model 3D software package, for an apex height of $h=0.57$ m. The optimal angle was found to be $\theta_{0,opt}=15$ deg, equal to the one computed previously. In Fig. 4 snapshots every 0.1 s are shown, together with the time plots of θ , l , for the optimal gait at point A in Fig. 3.

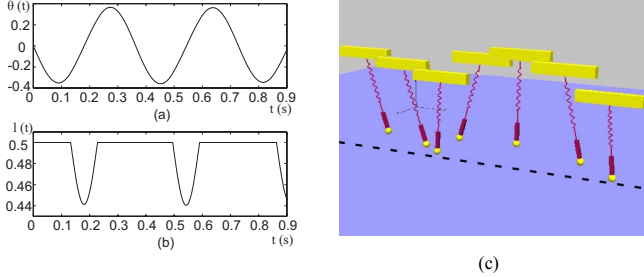


Fig. 4. Robot optimum gait, (a) θ , (b) l , (c) Working Model 3D motion snapshots.

To conclude, due to the approximations made, it is expected that Eq. (41) predicts the optimum $\theta_{0,opt}$ approximately. However, its main advantage is that it correctly predicts the qualitative effect of the parameters m , and k on the optimum angle, as demonstrated in Table 1, for a wide range of parameters. Also, the qualitative effect of the apex height h appears to be correctly predicted, as demonstrated by the example in Fig. 3.

VI. ACTUATOR - INDUCED LIMITATIONS

The motor used on the robot is described by the following torque-speed characteristic:

$$\tau_m = (Vk_m - \omega k_m^2) / r \quad (42)$$

where ω is the angular speed of the motor, and V is the voltage applied to the motor. The torque speed characteristic is shown in Fig.5, for some value of the applied voltage V and for the maximum voltage V_{max} . Due to the transformation constant g_e , the motor speed is:

$$\omega = g_e \dot{l} \quad (43)$$

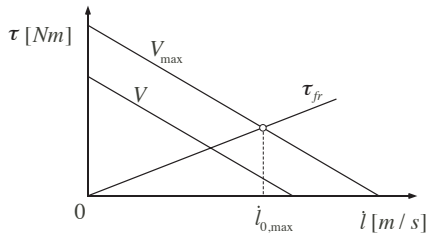


Fig. 5. Torque - speed characteristic of motor and curve of torque τ_{fr} required to compensate friction.

From Eqs. (3), and (5), the required motor torque τ_{fr} each moment so as to compensate friction is:

$$\tau_{fr} = b \cdot \dot{l} / g_e \quad (44)$$

and is shown in Fig. 5. On the other hand, from Eqs. (42), and (43), the torque the motor supplies at any point is:

$$\tau_m(\dot{l}, V) = (Vk_m - g_e \dot{l} \cdot k_m^2) / r \quad (45)$$

During normal operation, the motor supplies a torque

given by Eq. (45), which must be equal to the required torque to compensate friction, see Eq. (44). Therefore it is found that:

$$\dot{l} = Vk_m g_e / (b \cdot r + (k_m g_e)^2) \quad (46)$$

Eq. (46) expresses the relationship between the leg velocity l and the voltage V applied to the motor, when friction is being compensated. Since the leg velocity is greatest at touchdown, the friction force will also be greatest then. So if the motor is capable of compensating friction at touchdown, then it is always capable of compensating friction. At touchdown, Eq. (46) gives:

$$\dot{l}_0 = Vk_m g_e / (b \cdot r + (k_m g_e)^2) \quad (47)$$

Eq. (47) expresses the leg velocity that the robot may have at touchdown, for a given voltage V at touchdown, so that the motor may always compensate friction. In Fig. 5 this is the leg velocity for which the curve of the friction compensating torque intersects the torque - speed characteristic of the motor for an applied voltage of V . From Eq. (47), it may be seen that the greatest leg velocity the robot may have at touchdown is that which corresponds to the maximum voltage V_{max} :

$$\dot{l}_{0,max} = V_{max} k_m g_e / (b \cdot r + (k_m g_e)^2) \quad (48)$$

In Fig. 5 this is the leg velocity that corresponds to the intersection of the friction compensating torque with the torque - speed characteristic of the motor for the voltage V_{max} . This means that for a gait with leg velocity \dot{l}_0 greater than the critical value $\dot{l}_{0,max}$ the motor will be unable to supplement the energy losses.

Due to the condition of a symmetric stance phase, the critical value $\dot{l}_{0,max}$ corresponds to a critical gait with a certain angle $\theta_{0,crit}$, for a given apex height h . Therefore, the motor is unsuitable for any gait with an angle $\theta_0 > \theta_{0,crit}$ for the apex height h . This is because, for a given apex height h and for a symmetric stance phase, a gait with a greater angle θ_0 requires a greater \dot{l}_0 , as is evident from Eq. (36).

The critical angle $\theta_{0,max}$ may be smaller than the angle that would be optimal with an unlimited torque motor. In such cases $\theta_{0,max}$ is the optimal θ_0 , as larger values of θ_0 are not feasible. In Fig.6, this can be seen for a robot with $k=10000$ N/m, $m=10$ kg, $b=5$ kg/s, $k_m=0.04$ Nm/A, $g_e=20$ rad/m, $r=4 \Omega$, $V_{max}=48$ V, for $h=0.57$ m.

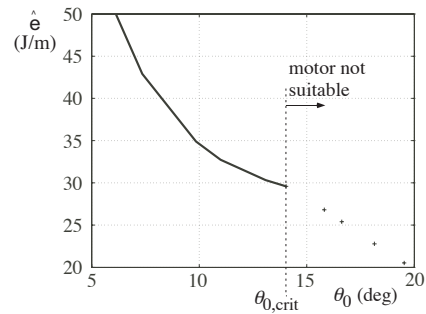


Fig. 6. Optimal θ_0 in the presence of a torque-limited motor.

VII. CONCLUSIONS

In this paper, it was shown that there exists a particular

passive gait, of all those possible, that leads to the least dissipated energy per meter of travel. The dynamics of the robot were approximated by a SLIP model. Certain assumptions were made to come to an analytical prediction for the optimal gait. The analytical prediction found is fairly accurate, and has a simple form that correctly predicts the qualitative behavior of all the parameters involved. Also, the accuracy of the analytical prediction has been verified with simulations of a complete robot model, including pitching of the body mass, as well as inertia in the leg. Finally, a model of a torque-limited actuator was included in the model. The analysis predicts which gaits are possible and whether the optimal gait can be achieved with a given motor.

REFERENCES

- [1] Raibert, M. H., "Legged Robots That Balance," *MIT Press*, Cambridge, MA, 1986.
- [2] Ahmadi, M. and Buehler, B., "Stable Control of a Simulated One-Legged Running Robot with Hip and Leg Compliance," *IEEE Transactions on Robotics & Automation*, Vol. 13, No. 1, February 1997.
- [3] Hodgins, J., "Legged Robots on Rough Terrain: Experiments in Adjusting Step Length," *Proc. of the 1988 IEEE Int. Conference on Robotics & Automation*, Philadelphia, Pennsylvania, April 1988, pp. 824-825.
- [4] Talebi, S., Poulakakis, I., Papadopoulos, E., and Buehler, "Quadruped Robot Running With a Bounding Gait," *Proc. of the Seventh Int. Symposium on Experimental Robotics (ISER'00)*, Honolulu, Hawaii, December 2000.
- [5] Simmons, R., Krotkov, E., "An Integrated Walking System for the Ambler Planetary Rover," *Proc. of the 1991 IEEE Int. Conference on Robotics & Automation*, Sacramento, California, April 1991, pp. 2086-2091.
- [6] Buehler, M., Koditschek, E., "Analysis of a Simplified Hopping Robot," *Proc. of the 1988 IEEE Int. Conference on Robotics & Automation*, Philadelphia, Pennsylvania, April 1988, pp. 817-819.
- [7] Dummer, R. and Berkemeier, M., "Low-Energy Control of a One-Legged Robot with 2 Degrees of Freedom," *Proc. of the 2000 IEEE Int. Conference on Robotics & Automation*, San Francisco, CA, April 2000, pp. 2815-2821.
- [8] Schwind, W. J., Koditschek, D. E., "Approximating the Stance Map of a 2-DOF Monoped Runner," *Journal of Nonlinear Science*, vol.10, pp. 533-568, 2000.
- [9] McGeer, T., "Passive dynamic walking," *Int. Journal of Robotics Research*, 9(2):62-82, April 1990.
- [10] Park, J. H., and Kim K. D., "Biped Robot Walking Using Gravity-Compensated Inverted Pendulum Mode and Computed Torque Control," *Proc. IEEE Int. Conference on Robotics & Automation*, Leuven, Belgium, May 1998, pp. 3528-3533.
- [11] Kajita, S., Kanehiro, F., Kaneko, K., Yokoi, K., and Hirukawa, H., "The 3D Linear Inverted Pendulum Mode: A simple modeling for a biped walking pattern generation," *Proc. of the 2001 IEEE/RSJ Int. Conference on Intelligent Robots and Systems*, Maui, Hawaii, USA, Oct.-Nov. 2001, pp. 239-246.
- [12] Schwind, W. J., Koditschek, D. E., "Control of Forward Velocity for a Simplified Planar Hopping Robot," *Proc. of the 1995 IEEE Int. Conference on Robotics & Automation*, Nagoya, Aichi, Japan, pp.691-696, 1995.
- [13] Poulakakis, I., Papadopoulos, E., Buehler, M., "On the Stable Passive Dynamics of Quadrupedal Running," *Proc. of the 2003 IEEE Int. Conference on Robotics & Automation*, Taipei, Taiwan, pp.1368-1373, Sept. 2003.

APPENDIX A

For small θ , the equations of motion in Eq. (13) may be linearized:

$$\begin{aligned} L\ddot{\theta} - g\theta &= 0 \\ m\ddot{l} + k(l - L) + mg &= 0 \end{aligned} \quad (A1)$$

The solutions to Eqs. (A1) are:

$$\begin{aligned} \theta &= c_1 e^{a_6 t} + c_2 e^{-a_6 t} \\ l(t) &= \frac{mg}{k} \cos\left(\sqrt{\frac{k}{m}} t\right) + \sqrt{\frac{m}{k}} \dot{l}_0 \sin\left(\sqrt{\frac{k}{m}} t\right) + L - \frac{mg}{k} \end{aligned} \quad (A2)$$

$$a_6 = \sqrt{g/L}$$

where:

$$\begin{aligned} c_1 &= \theta_0/2 + \dot{\theta}_0/2a_6 \\ c_2 &= \theta_0/2 - \dot{\theta}_0/2a_6 \end{aligned} \quad (A3)$$

Differentiating $l(t)$ in Eq. (A2), yields:

$$\dot{l}(t) = \dot{l}_0 \cos\left(\sqrt{k/m} \cdot t\right) - g\sqrt{m/k} \sin\left(\sqrt{k/m} \cdot t\right) \quad (A4)$$

Halfway during a symmetric stance phase, it is:

$$\dot{l}(T_s/2) = 0 \quad (A5)$$

Solving Eq. (A5) for T_s by using Eq. (A4), it is:

$$T_s = 2\sqrt{m/k} \left(-\arctan\left(-\dot{l}_0 \sqrt{k/m} / g\right) + \pi \right) \quad (A6)$$

Because $k/m \gg 1s^{-2}$, the following are true:

$$\arctan\left(-\dot{l}_0 \sqrt{k/m} / g\right) \cong \pi/2 \quad (A7)$$

$$T_s = \pi\sqrt{m/k} \quad (A8)$$

APPENDIX B

For a symmetric motion, the following is true:

$$\theta(T_s/2) = 0 \quad (B1)$$

Taking into account Eq. (A2) and Eq. (B1), we have:

$$a_6 \theta_0 / \dot{\theta}_0 = \left(1 - e^{2a_6 T_s/2}\right) / \left(1 + e^{2a_6 T_s/2}\right) \quad (B2)$$

Taking into account Eq. (A8), Eq. (B2) is of the form:

$$a_6 \theta_0 / \dot{\theta}_0 = \left(1 - e^{2x}\right) / \left(1 + e^{2x}\right) = f_1(x) \quad (B3)$$

where $x = \pi\sqrt{mg/(4kL)}$.

For realistic cases, the max value of x is 0.35. Plotting $f_1(x)$ and $f_2(x) = -x$ in Fig. 7, it can be seen that $f_1(x) \approx f_2(x)$. Due to this fact, and substituting for x , it is found that:

$$\dot{\theta}_0 = -\theta_0 2\sqrt{k/(m\pi^2)} \quad (B4)$$

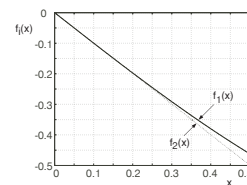


Fig. 7. Functions f_1 and f_2 .